Discrete Alfvén eigenmodes in international thermonuclear experimental reactor operations with negative magnetic shear*

Wang Jun(王 军)†, Hu Shuang-Hui(胡双辉)‡, Dai Qing-Ping(代清平)[a)], and Yao Long-Bao(姚龙宝)

College of Science, Guizhou University, Guiyang 550025, *China*

(Received 18 December 2009; revised manuscript received 19 February 2010)

Discrete Alfvén eigenmodes in steady-state operation scenarios with negative magnetic shear in the international thermonuclear experimental reactor are investigated in this paper. These magnetohydrodynamic eigenmodes are trapped by the α-induced potential wells along the magnetic field line. Here $\alpha = -q^2 R \mathrm{d}\beta/\mathrm{d}r$ with q being the safety factor, β the ratio between plasma and magnetic pressures, and R the major radius, and r the minor radius. Due to negligible continuum damping via wave energy tunneling, these Alfvén eigenmodes could be readily destabilized by energetic particles.

Keywords: Alfvén eigenmodes, negative magnetic shear, magnetohydrodynamic instability
PACC: 5235B, 5255G, 5235P

1. Introduction

Since Hannes Alfvén discovered Alfvén waves in 1942,[1] these waves have been found to play an important role in the dynamics of magnetised plasmas. It has been realised that Alfvén modes could be a serious threat to the classical confinement of energetic particles in tokamak plasmas. Significant progress has been achieved in both theoretical and experimental studies of Alfvén modes. Various eigenmodes have been observed and identified in experiments, such as toroidal-induced Alfvén eigenmode (TAE),[2] energetic-partical continuum mode (EPM),[3] and so on. Nowadays Alfvén waves are also important in fusion plasmas.[4−6] Tokamak fusion research has been progressed into negative magnetic shear regime, e.g. JT 60-U, JET, DIII-D and the international thermonuclear experimental reactor (ITER). The ITER is an important step on the road to fusion power plants. It is designed as an experimental device with extensive diagnostics and considerable flexibility in fusion power, and will be the first fusion device with significant Q (the ratio of fusion power to heating power). Several steady state operation scenarios are designed for the ITER. Some of them operate with negative magnetic shear.[7−9] Since Alfvén waves in fusion plasmas are very important, different types of Alfvén eigenmodes are investigated in the ITER. The α-induced toroidal Alfvén eigenmode (αTAE),[10] where $\alpha = -q^2 R \mathrm{d}\beta/\mathrm{d}r$ with q being the safety factor, β the ratio between plasma and magnetic pressures, and R the major radius, and r the minor radius, is one type of discrete Alfvén eigenmodes, which are trapped in ballooning-drive potential wells in toroidal plasmas. These modes present a potential danger to fusion reactors because they can eject high energy alpha particles from the plasmas before their thermalisation. These particles can carry considerable energy that may damage the first wall of reactors. We, thus, are motivated to investigate the stability features of discrete Alfvén eigenmodes in steady state operation scenarios with negative magnetic shear in the ITER. We have in mind the (s, α) model equilibrium,[11] with $s = r(\mathrm{d}q/\mathrm{d}r)/q$ being the magnetic shear.

The rest of this paper is organised as follows. The basic model is presented in Section 2. The result and analysis are displayed in Section 3. In Section 4 we give the conclusions.

2. Basic model

We adopt the ballooning mode formalism[12,13] and the (s, α) model equilibrium[11] for an axisymmetric toroidal plasma with a large aspect ratio (i.e.,

*Project supported by the National Natural Science Foundation of China (Grant No. 10675037).
†Corresponding author. E-mail: 78334062@qq.com
‡E-mail: sci.shhu@gzu.edu.cn
© 2010 Chinese Physical Society and IOP Publishing Ltd

$\varepsilon = r/R << 1$) and shifted circular magnetic surface in the ideal magnetohydrodynamic (MHD) description. The high-n shear Alfvén wave is then governed by the vorticity equation,

$$\mathrm{d}^2\delta\phi/\mathrm{d}\theta^2 + \Omega^2(1 + 2\varepsilon_0\cos\theta)\delta\phi - V(\theta)\delta\phi = 0, \quad (1)$$

where $\Omega = \omega/\omega_\mathrm{A}$, $\omega_\mathrm{A} = v_\mathrm{A}/qR$ with v_A being the Alfvén speed, $\varepsilon_0 = 2\ (\varepsilon + \mathrm{d}\Delta/\mathrm{d}r)$, Δ is the Shafranov shift, $f = 1 + (s\theta - \alpha\sin\theta)^2$, and $V(\theta)$ is the potential given by

$$V = (s - \alpha\cos\theta)^2/f^2 - \alpha\cos\theta/f \quad (2)$$

with $-\infty < \theta < \infty$ being the extended poloidal angle coordinate along the magnetic field.

Physical eigenmodes can be obtained by solving Eq. (1) with appropriate boundary conditions. From Eq. (2), we have $V \to O(1/\theta^2)$ as $|\theta| \to \infty$. Thus, for large $|\theta|$, Eq. (1) asymptotically reduces to the standard Mathieu's equation. According to Floquet's theorem, its solution is represented by $\delta\phi = \exp(\mu\theta)M(\theta)$, where μ is a complex number and $M(\theta)$ is a periodic function. The αTAE solution is obtained with the help of the causality boundary condition. In the ideal MHD stable domain, this condition corresponds to the outgoing wave boundary conditions and, thus, makes it able to describe tunneling leakage of wave energy. Equation (1) is then solved by a numerical shooting code incorporating the boundary conditions.[10]

3. Results and analysis

There are several steady state operation scenarios of ITER with negative magnetic shear. The internal transport barrier (ITB) appears in the discharges with negative magnetic shear. We study two typical cases in this paper. In the first case we choose the plasma parameter profile at the current flat-top phase ($t > 1000$ s) for the weak negative magnetic shear (WNS) operation scenario.[7] The safety factor profile in this scenario is similar to those in ITB experiments of other tokamaks. We focus on the negative magnetic shear regime, corresponding to the normalised minor radius range of 0.5–0.65. The associated s and α vary in ranges of $[-0.6, 0]$ and $[1, 2.5]$, respectively.

Numerical results demonstrate that αTAEs can indeed be trapped in the α-induced potential wells in the negative magnetic shear case. The potential structures are displayed in Fig. 1(a). A complex eigenmode frequency, $\Omega = \Omega_\mathrm{r} + \mathrm{i}\,\Omega_\mathrm{i} = 0.713 - \mathrm{i}\,5.88 \times 10^{-6}$, is obtained for the αTAE with an even parity. The corresponding eigenmode structures are shown in Fig. 1(b). The eigenmode is trapped in potential wells. The negative Ω_i indicates a small damping rate for energy leakage via tunneling through the potential barriers, shown in Fig. 1(a). The αTAE is a quasi-marginally stable mode and can even survive without the toroidal Alfvén frequency gap. The αTAE can also exist with an odd parity. Figure 1(c) shows the odd eigenmode structures. The corresponding complex eigenmode frequency is $\Omega = \Omega_\mathrm{r} + \mathrm{i}\,\Omega_\mathrm{i} = 0.9595 - \mathrm{i}\,5.02 \times 10^{-4}$. It is a higher-order eigenstate next to the even αTAE, shown in Fig. 1(b). The out-going wave nature is indicated by phase difference between the real and imaginary components of $\delta\phi$. We can see that the eigenmode is well trapped in the wells.

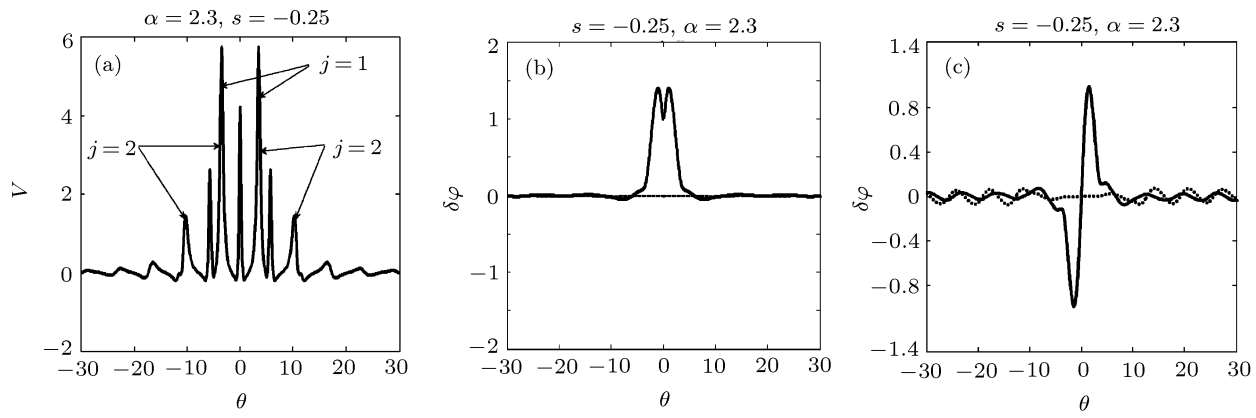


Fig. 1. (a) Potential V versus θ, (b) even eigenmode structures versus θ, (c) and odd eigenmode structures versus θ for $\varepsilon_0 = 0.2$, $s = -0.25$, and $\alpha = 2.3$. Solid and dot lines are, respectively, real and imaginary components in both (b) and (c).

As α increases, the real frequency of eigenmodes will increase. Figure 2(a) shows the dependence of the even-parity eigenmode frequency on ballooning driving term by α for $\varepsilon_0 = 0.2$, $s = -0.25$. It is independent of toroidal Alfvén frequency gap, denoted by the two dot-dash lines . When α is bigger than 1.4, the eigenmodes are out of the toroidal Alfvén frequency gap. Odd-parity eigenmode frequencies are shown in Fig. 2(b). Higher frequencies are also observed for these odd modes in the negative magnetic shear case.

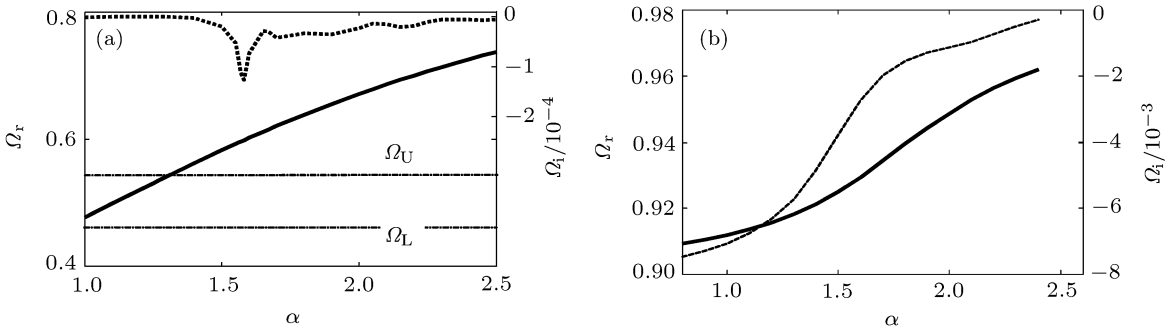


Fig. 2. (a) Even-parity eigenmode frequencies (Ω_U and Ω_L denote the toroidal Alfvén frequence gap) and (b) odd-parity eigenmode frequencies versus α for $\varepsilon_0 = 0.2$, $s = -0.25$. The solid line and dot line represent the real and the imagine parts, respectively.

We plot the potential and the eigenmode structures for $s = -0.25$ and $\alpha = 1.57$ in Fig. 3(a). The corresponding complex eigenmode frequency is $\Omega = \Omega_r + \mathrm{i}\,\Omega_i = 0.596 - \mathrm{i}\,1.123 \times 10^{-4}$. The case for $s = -0.25$ and $\alpha = 2$ is displayed in Fig. 3(b). The corresponding complex eigenmode frequency is $\Omega = \Omega_r + \mathrm{i}\,\Omega_i = 0.67 - \mathrm{i}\,2.23 \times 10^{-5}$. We can see that the damping rate of waves (absolute value of the imagine part of the mode complex frequency) becomes small as α increases. The reason is that as α increases, the potential well becomes deeper as shown in Fig. 3(c). The deeper potential well can better trap the eigenmodes so that the damping rate decreases as α increases.

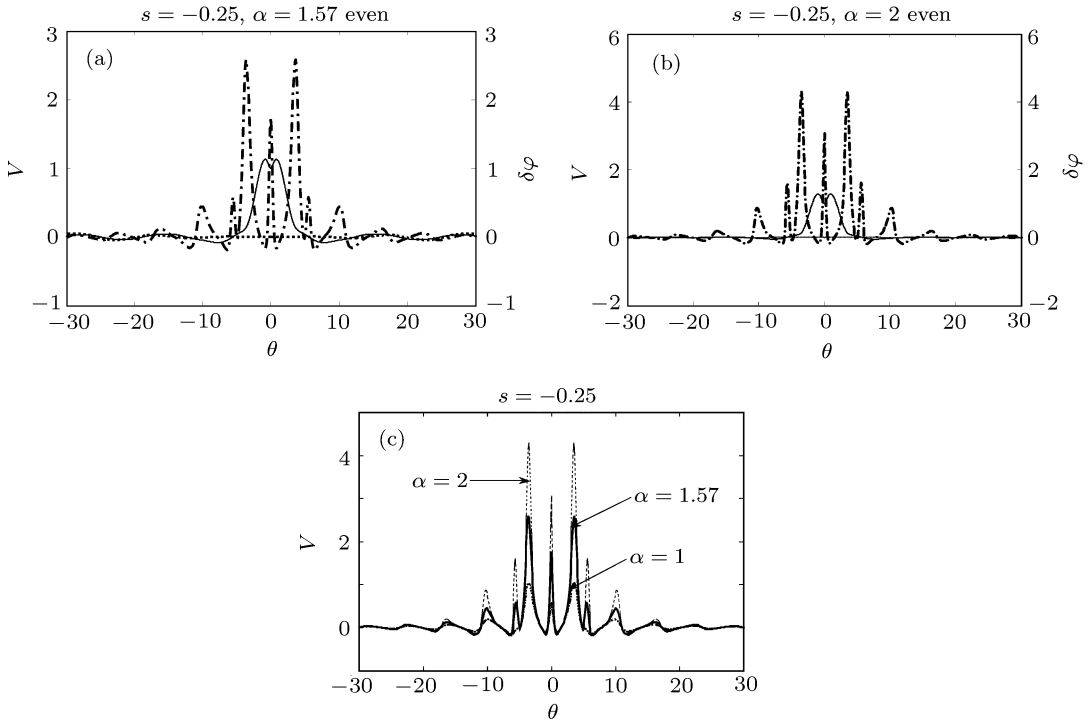


Fig. 3. (a) Potential and eigenmode structures for $s = -0.25$ and $\alpha = 1.57$; (b) potential and eigenmode structures for $s = -0.25$ and $\alpha = 2$ (the solid line represents the real part of $\delta\phi$, the dot line refers to the imagine part of $\delta\phi$, and the dot-dash line denotes the structure of potential), and (c) the potential structures for $s = -0.25$ with $\alpha = 1.0$ (dot-dash line), 1.57 (solid line), and 2.0 (dot line).

From Figs. 4(a)–4(c), we can see that the mode damping rate becomes small as the absolute value of s decreases. The reason is that as the absolute value of s decreases, the potential well becomes deeper, which is shown in Fig. 4(d). The deeper potential well can better trap the eigenmodes so that the damping rate decreases as the absolute value of s decreases.

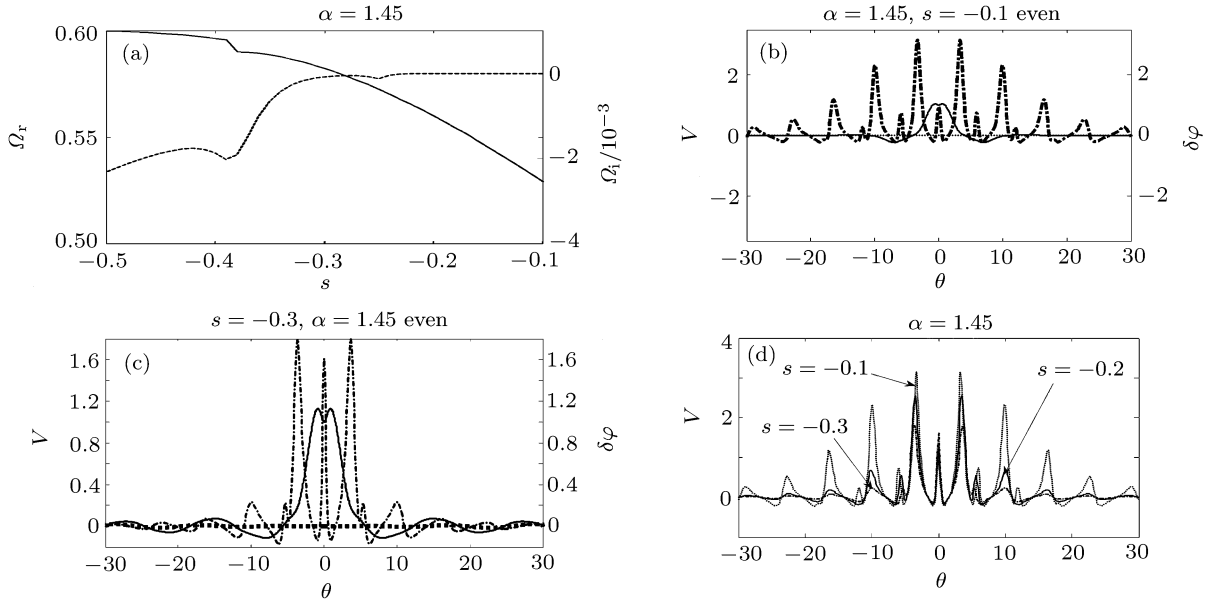


Fig. 4. (a) Even-parity eigenmode frequencies versus s for $\varepsilon_0 = 0.2$ and $\alpha = 1.45$; (b) potential and eigenmode structures for $s = -0.1$; (c) potential and eigenmode structures for $s = -0.3$ (in panels (b) and (c), the solid line is the real part of $\delta\phi$, the dot line is the imagine part of $\delta\phi$, and the dot-dash line is the potential); (d) the potential structures for $\alpha = 1.45$, with $s = -0.1$ (dot line), -0.2 (solid line), and -0.3 (dot-dash line).

The other steady-state operation scenario is for the case where an internal transport barrier exists.[8] It is a long time(> 3000 s) steady-state discharge with negative magnetic shear. In this case the absolute value of s is higher than that in the first case. From Figs. 5(a)–5(c), we can see that for $s = -0.8$ and $\alpha = 4$ there indeed exist discrete Alfvén eigenmodes with small damping rates. They are well trapped in the potential wells.

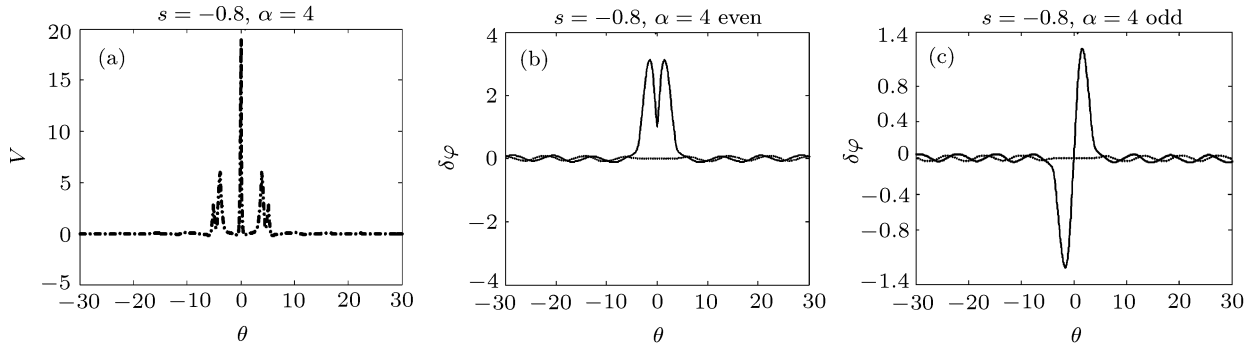


Fig. 5. (a) Potential structures versus θ; (b) even eigenmode structures versus θ; (c) odd eigenmode structures versus θ for $\varepsilon_0 = 0.2$, $s = -0.8$, and $\alpha = 4$. The solid line represents the real part of $\delta\phi$, the dot line refers to the imagine part of $\delta\phi$ in both panels (b) and (c).

We use parameters s and α in the high $|s|$ operation to investigate the stability features of the discrete Alfvén eigenmodes for this long-time steady state operation scenario. First, we scan s for $\alpha = 3.5$ and plot the even and the odd eigenmode frequencies in Fig. 6(a) and 6(c), respectively. We then scan α for $s = -0.8$ and display the even and the odd eigenmode frequencies in Figs. 6(b) and 6(d), respectively. We can see that there

exist plenty of discrete Alfvén eigenmodes in this scenario.

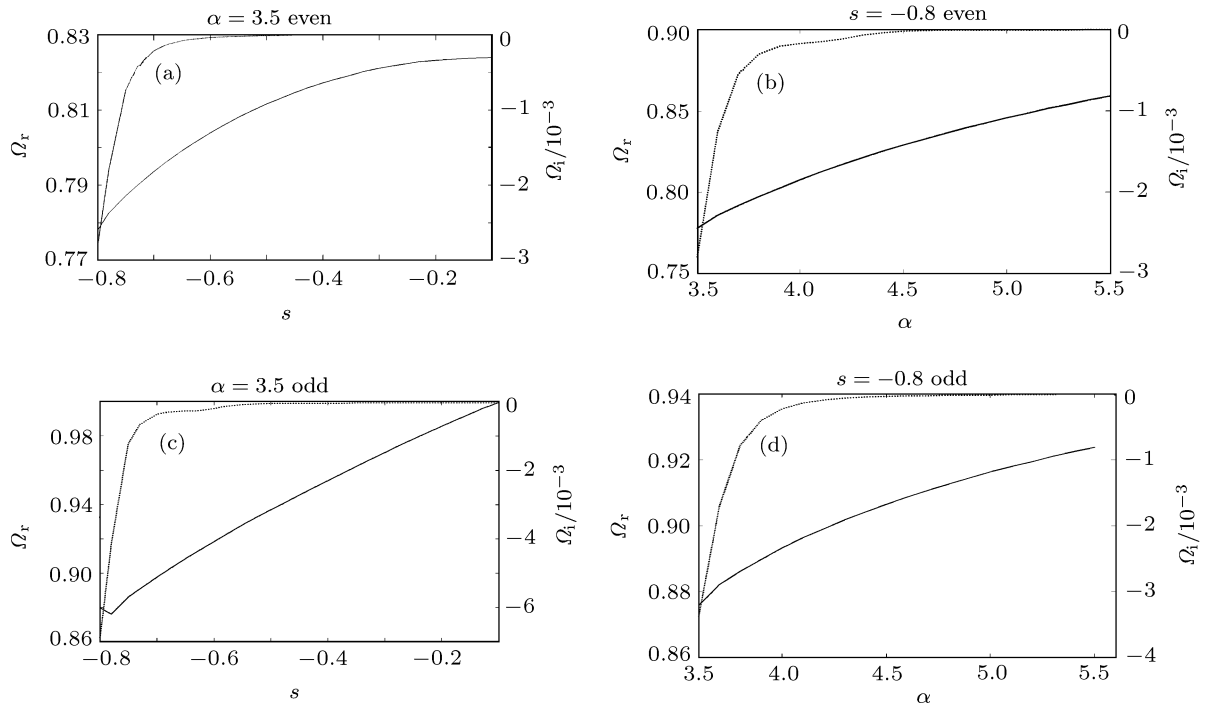


Fig. 6. (a) Even-parity eigenmode frequencies versus s for $\alpha = 3.5$; (b) even-parity eigenmode frequencies versus α for $s = -0.8$; (c) odd-parity eigenmode frequencies versus s for $\alpha = 3.5$; (d) odd-parity eigenmode frequencies versus α for $s = -0.8$. $\varepsilon_0 = 0.2$ is used for all the four cases. The solid and the dot lines represent real and imaginary components, respectively.

We have studied the discrete Alfvén eigenmodes and presented the stability features in the two steady state operation scenarios. There exist plenty of αTAEs, which are quasi-marginally stable. They could, thus, be readily excited by energetic particles and become unstable. Therefore, the αTAE is important in ITER operation with negative magnetic shear.

4. Conclusions

Based on the ideal MHD description and the (s, α) tokomak model equilibrium, we investigate the αTAE in two typical operation scenarios of ITER with negative magnetic shear. There exist plenty of discrete Alfvén eigenmodes in both typical cases. We study the stability features of the eigenmode in these scenarios. We can see that the discrete Alfvén eigenmodes in negative magnetic shear cases are similar to the positive magnetic shear case. They are independent of the toroidal Alfvén frequency gap, and they are also trapped in α-induced potential wells with negligible tunneling damping rate. These quasi-marginally stable eigenmodes could be readily driven to be unstable by energetic particles. Therefore, our studies indicate that these discrete Alfvén eigenmodes are important in the ITER operations with negative magnetic shear.

References

[1] Alfvén H 1942 *Nature* **150** 405

[2] Cheng C Z, Chen L and Chance M S 1985 *Ann. Phys.* N.Y. **161** 21

[3] Chen L 1994 *Physics of Plasmas* **1** 1519

[4] Heidbrink W W 2008 *Physics of Plasmas* **15** 055501

[5] Podestà M and Heidbrink W W 2009 *Physics of Plasmas* **16** 056104

[6] Jian G D and Dong J Q 2005 *Acta Phys. Sin.* **54** 1641 (in Chinese)

[7] ITER Technical Basis 2001 GAO FDR 1 00-07-13 R1.0 (Vienna: IAEA) Section 4.3.3 p11

[8] Garcia J, Giruzzi G, Artaud J F, Basiuk V, Decker J, Imbeaux F, Peysson Y and Schneider M 2008 *Plasma Phys. Control. Fusion* **50** 124032

[9] Houlberg W A, Gormezano C, Artaud J F, Barbato E, Basiuk V, Becoulet A, Bonoli P, Budny R V, Eriksson L G, Farina D, Gribov Yu, Harvey R W, Hobirk J, Imbeaux F, Kessel C E, Leonov V, Murakami M, Polevoi A, Poli E, Prater R, John H St, Volpe F, Westerhof E, Zvonkov A, ITPA Steady State Operation Topical Group and ITPA Confinement Database and Modeling Topical Group 2005 *Nucl. Fusion* **45** 1309

[10] Hu S and Chen Liu 2004 *Physics of Plasmas* **11** 1

[11] Connor J W, Hastie R J and Taylor J B 1978 *Phys. Rev. Lett.* **40** 396

[12] Lee Y C and van Dam J W 1979 *Proceedings of the Finite Beta Theory Workshop* (Washington: U.S. DOE) p93

[13] Connor J W, Hastie R J and Taylor J B 1979 *Proc. R. Soc. London Ser.* A **365** 1